Two-state folding of the outer membrane protein X into a lipid bilayer membrane

Parthasarathi Rath, Timothy Sharpe, Bastian Kohl, and Sebastian Hiller*

Biozentrum, University of Basel, 4056 Basel, Switzerland

*Correspondence: sebastian.hiller@unibas.ch

Abstract

Folding and insertion of β-barrel membrane proteins into native membranes is efficiently catalyzed by β-barrel assembly machineries. Understanding this catalysis requires a detailed description of the corresponding uncatalyzed folding mechanisms, which however have so far remained largely unclear. Here, we resolve folding and membrane insertion of the *E. coli* outer membrane protein X (OmpX) into 1,2-didecanoyl-sn-glycero-3-phosphocholine (PC10:0) membranes at the atomic level. By combining four different experimental techniques, we correlate global folding kinetics with global and local hydrogen bond formation kinetics. Under a well-defined reaction condition, these processes follow single-exponential velocity laws, with rate constants identical within experimental error. The data thus establish at atomic resolution that OmpX folds and inserts into the lipid bilayer of PC10:0 liposomes by a two-state mechanism.

In Gram-negative bacteria, mitochondria and chloroplasts, β-barrels are the predominant architectural class of proteins in the outer membranes, facilitating essential physiological functions.[1] Improper targeting and misfolding hampers cell physiology, leads to aggregation phenotypes and associated diseases.[2] Bacterial cells duplicate their entire outer membrane in as short as 20 minutes and outer membrane protein (OMP) folding *in vivo* must therefore occur on a substantially shorter time scale, i.e. on the order of seconds or faster. To achieve such fast kinetics, folding and insertion of OMPs *in vivo* is catalyzed by the β-barrel assembly machinery (BAM).[3] Understanding this fundamental catalysis step of OMP biogenesis essentially requires to study the uncatalyzed reaction, *i.e.* the BAM-independent folding mechanism as a reference point.

BAM-independent folding and insertion of OMPs into lipid bilayers *in vitro* has been studied extensively, but no clear mechanistic concept has so far emerged.[4] For the smallest OMPs with 8 strands, two fundamentally different folding mechanisms have so far been described. On the one hand, the folding of OmpA into lipid bilayers has been shown to follow a slow and coherent process via multiple intermediate steps, the so-called "concerted insertion mechanism".[4e] This mechanism has recently been refined to include up to nine intermediate states.[4b] Notably, this mechanism has so far not been resolved by high-resolution methods and the nature of the intermediate states is therefore unclear. On the other hand, the 8-stranded protein PagP was shown to fold by a two-state mechanism under highly denaturing conditions of 8M urea solution.[4c] Point mutations and φ_F-value analysis suggested a tilted transition state in the lipid bilayer membrane. Notably, the two-state behavior was observed under highly denaturing concentrations and the study therefore does not allow conclusions on the presence or absence of intermediate states under physiological conditions.

We therefore deem it necessary to study an OMP insertion process with high-resolution methods under non-denaturing conditions. We have previously established a technical setup to monitor the formation of β-barrel hydrogen bonds at the single residue level by hydrogen/deuterium (H/D) exchange in combination with mass spectrometry and solution NMR spectroscopy.[5] This technical setup has the potential to not only detect folding intermediates, but also to characterize them structurally. Here, we apply these techniques

to characterize folding of the 8-stranded β-barrel OmpX from *E. coli* into a lipid bilayer membrane at the atomic level.

As a starting point, the global kinetics of OmpX folding into homogeneous PC10:0 liposomes were determined by two bulk methods, SDS-PAGE gel shift assay and tryptophan fluorescence spectroscopy. Folding was studied at pH 10.0 and in the presence of 600 mM arginine. Arginine is known to solubilize unfolded proteins, preventing their aggregation, but is not a chaotropic denaturant.[6] The elevated pH, in turn, assures rapid solvent exchange for accessible amide protons.[7] On the SDS-PAGE gel the folded and unfolded species of OmpX can be readily distinguished by the characteristic band shift for folded OMPs (Figure 1A). Starting from completely unfolded protein, after around 10 minutes the OmpX folding reaction has essentially completed. The fraction of folded OmpX as a function of folding time T follows a single exponential with folding rate constant of $k_F = 0.0098 \pm 0.00042$ s^{-1} (Figure 1B). As a second method, we monitored the same folding process under identical buffer conditions by real-time tryptophan fluorescence spectroscopy. OmpX contains two tryptophan residues at amino acid position 76 and 140 located in the periplasmic turn 2 and in strand 8 (Figure S1). Upon folding, the fluorescence spectrum experiences a characteristic blue shift with an increase in fluorescence intensity (Figure 1C). The fluorescence intensity at 340 nm as a function of the folding time T follows a single exponential with folding rate constant of $k_F = 0.010 \pm 0.00014$ s^{-1} (Figure 1D).

The three-dimensional structure of a β-barrel membrane protein is defined by a network of backbone hydrogen bonds between adjacent strands around the entire barrel circumference.[8] Their formation provides a key factor stabilizing the protein in the low dielectric and apolar membrane environment.[9] We used H/D-exchange in a pulsed quenched flow setup to monitor hydrogen bond formation during folding of OmpX into lipid bilayers. In our custom-built apparatus, complete OMP folding into liposomes was achieved with simultaneous incorporation of deuterons at non-exchangeable amide positions at variable folding time T (Figure S2). To enable the observation of individual resonances of OmpX by solution NMR spectroscopy, the refolded protein was transferred from proteoliposomes into N,N-dimethyldodecylamine N-oxide (LDAO) micelles after completion

of the folding reaction (Figure S3A). OmpX stays folded during this transfer, as evidenced by the observation that protein refolded in D_2O-buffer into liposomes preserves its deuterium content in the barrel core into micelles (Figure S3B). Furthermore, amide proton back-exchange in the core of the folded protein occurs with kinetics on the timescale of tens of days[5] so that its contributions are negligible during the few hours that are needed for sample preparation. The resulting 2D [^{15}N, ^{1}H]-TROSY NMR spectrum of OmpX in LDAO micelles is well-dispersed, and facilitates sequence-specific quantification of deuterium incorporation as a function of folding time T (Figure 2A). During the preparation of the time zero ($T = 0$ s) sample, the deuterated protein is transferred into H_2O-buffer before it can even fold and it then refolds in the H_2O-buffer. Hence, all amide signals are observed with maximal intensity. On the other end of the timescale, at very large T, the protein is transferred to H_2O-buffer only after folding has essentially completed in D_2O-buffer. Therefore, all amide protons that are exchange-protected in the barrel structure show a decrease of the NMR signal as a function of the folding time T (Figure 2B–E). In contrast, amide protons that are rapidly exchanging in the folded state of OmpX feature constant NMR signal intensities irrespective of folding time T. This is exemplified for the residues G16 and N19 located in the first extracellular loop of OmpX (Figure 2B–C). For each of the exchange-protected residues, the decrease in amide proton NMR signal intensities as a function of T was found to be well described by a single exponential function, yielding the residue-specific hydrogen bond formation rate constant $k_H(i)$. These were all found to be identical within the experimental error, averaging to 0.014 ± 0.0048 s^{-1} (Figure 2C and 2D).

As a fourth method to determine the hydrogen incorporation per molecule, we quantified H/D exchanged samples obtained with the pulsed quenched flow setup by Electrospray Ionization Time-of-Flight (ESI-TOF) mass spectrometry (Figure S4A).[5, 10] Also in this method, protons in flexible parts exchange rapidly with solvent protons during sample preparation and only amide protons in the barrel core retain their deuterium content. Undesirable back-exchange during the injection and in the gas phase of the ESI-MS experiments was minimized by using water-free organic solvents and rapid sample handling. Consequently, deconvolution of signal resulted in clearly distinguishable signals for the barrel-protonated and barrel-deuterated OmpX molecules with respective masses of 16390 and 16430 Da (Figure 3). Superposition of the deconvoluted spectra for each sampled folding time point T

directly shows a bimodal population shift from the fully protonated to the fully deuterated OmpX species, without any intermediate species (Figure 3A), demonstrating the absence of any intermediate state during the transition from unfolded to folded OmpX and the formation of the entire hydrogen bonding network in a single, cooperative event. The fraction of deuterated OmpX as a function of folding time T follows a single exponential with hydrogen bond formation rate constant of $k_H = 0.012 \pm 0.0007$ s^{-1} (Figure 3B).

Taken together, the folding of OmpX into a PC10:0 lipid bilayer membrane was resolved by four different experimental methods, fluorescence spectroscopy, SDS-PAGE, and H/D-exchange coupled to NMR spectroscopy and mass spectrometry. The four methods deliver the global folding rate constant k_F, and the global and the residue-specific rate constants of hydrogen-bond formation, k_H and $k_H(i)$, respectively. For all four methods the data followed a single exponential law with rate constants on the minutes time scale and these are identical within experimental error (Table 1). The folding process is thus fully described by a two-state folding mechanism and the absence of any significantly populated intermediates. Unfolded OmpX inserts and folds from a membrane-associated state into the membrane with a single and irreversible structural rearrangement, resulting the native β-barrel structure. Hence, formation of the hydrogen bond network appears cooperative on the timescale of global folding.

This mechanism of insertion and folding of OmpX into PC10:0 bilayer is distinct from the concerted insertion mechanism reported previously for the similarly-sized protein OmpA, which progresses slowly and concertedly along multiple intermediate states.[4b, 4e] The apparent slow folding of bulk OmpX is a statistically rare, but not a microscopically slow process. Importantly, the available data do not resolve whether the actual formation of the hydrogen bond network of a single molecule of OmpX is cooperative or sequential. Finally, the mechanism agrees with the 2-state folding as observed for the protein PagP,[4c] however it is now established for the first time under non-denaturing conditions.

Notably, the mechanism established here is also in agreement with single-molecule studies of OMP folding by atomic force microscopy (AFM).[11] In these experiments, bilayer-embedded OMPs on a mica surface are subjected to a tensile load, resulting in stepwise

unfolding β-hairpin by β-hairpin. Thereby, a partially unfolded OMP with some of its hairpins left in the membrane refolds back to its native barrel conformation on a time scale of a few seconds.[11a, 11b, 12] Connecting these observations, it is tempting to speculate that also in the unperturbed refolding experiments the transmembrane crossing of a single hairpin would provide a seed sufficient for the rapid folding of the rest of the barrel. Consequently, the facilitation of such a single transmembrane crossing would then also be a sufficient mechanism for catalytic insertion by the BAM machinery.

In summary, we have established here at the atomic level that the membrane protein OmpX folds under certain non-denaturing condition into a lipid bilayer as a two-state process, where folding, insertion and hydrogen bond formation synchronously follow a single exponential velocity law. OmpX folding is microscopically a rare, not a slow process. This mechanistic description forms a well-defined starting point to address the folding mechanisms of OMPs under different conditions including (i) other OMPs with higher β-strand number, (ii) bilayers with longer lipid chain length, (iii) BAM-catalyzed folding under physiological conditions including the contributions of periplasmic chaperones. The fact that BAM-mediated folding is a prime target for novel antibiotics adds to the relevance of these findings.

Author Contributions
P.R. and S.H. designed the study, analyzed the data, and wrote the manuscript. P.R. and T.S. performed and analyzed the fluorescence experiments. B.K. performed control experiments. P.R. performed all other experiments. All authors commented on and approved the manuscript.

Experimental Section
The experimental section is included in the supplemental material.

References

[1]   a) S. K. Buchanan, *Curr. Opin. Struct. Biol.* **1999**, *9*, 455-461; b) R. Koebnik, K. P. Locher, P. Van Gelder, *Mol. Microbiol.* **2000**, *37*, 239-253; c) S. A. Paschen, W. Neupert, D. Rapaport, *Trends. Biochem. Sci.* **2005**, *30*, 575-582; d) S. Reumann, K. Inoue, K. Keegstra, *Mol. Membr. Biol.* **2005**, *22*, 73-86.

[2]   a) R. Di Maio, P. J. Barrett, E. K. Hoffman, C. W. Barrett, A. Zharikov, A. Borah, X. Hu, J. McCoy, C. T. Chu, E. A. Burton, T. G. Hastings, J. T. Greenamyre, *Sci. Transl. Med.* **2016**, *8*, 342ra378; b) H. Nikaido, *Antimicrob. Agents. Chemother.* **1989**, *33*, 1831-1836; c) C. R. Sanders, J. K. Myers, *Annu. Rev. Biophys. Biomol. Struct.* **2004**, *33*, 25-51; d) K. Sasaki, R. Donthamsetty, M. Heldak, Y. E. Cho, B. T. Scott, A. Makino, *Am. J. Physiol. Cell. Physiol.* **2012**, *303*, C1055-1060.

[3]   a) Y. Gu, H. Li, H. Dong, Y. Zeng, Z. Zhang, N. G. Paterson, P. J. Stansfeld, Z. Wang, Y. Zhang, W. Wang, C. Dong, *Nature* **2016**, *531*, 64-69; b) M. G. Iadanza, A. J. Higgins, B. Schiffrin, A. N. Calabrese, D. J. Brockwell, A. E. Ashcroft, S. E. Radford, N. A. Ranson, *Nat. Commun.* **2016**, *7*, 12865; c) C. T. Webb, E. Heinz, T. Lithgow, *Trends. Microbiol.* **2012**, *20*, 612-620; d) T. Wu, J. Malinverni, N. Ruiz, S. Kim, T. J. Silhavy, D. Kahne, *Cell* **2005**, *121*, 235-245.

[4]   a) N. K. Burgess, T. P. Dao, A. M. Stanley, K. G. Fleming, *J. Biol. Chem.* **2008**, *283*, 26748-26758; b) E. J. Danoff, K. G. Fleming, *Biochemistry* **2017**, *56*, 47-60; c) G. H. Huysmans, S. A. Baldwin, D. J. Brockwell, S. E. Radford, *Proc. Natl. Acad. Sci. U. S. A.* **2010**, *107*, 4099-4104; d) J. H. Kleinschmidt, *Biochim. Biophys. Acta.* **2015**, *1848*, 1927-1943; e) J. H. Kleinschmidt, T. den Blaauwen, A. J. Driessen, L. K. Tamm, *Biochemistry* **1999**, *38*, 5006-5016; f) J. H. Kleinschmidt, L. K. Tamm, *Biochemistry* **1996**, *35*, 12993-13000; g) J. H. Kleinschmidt, L. K. Tamm, *Biochemistry* **1999**, *38*, 4996-5005.

[5]   T. Raschle, P. Rios Flores, C. Opitz, D. J. Muller, S. Hiller, *Angew. Chem. Int. Ed. Engl.* **2016**, *55*, 5952-5955.

[6]   a) T. Arakawa, D. Ejima, K. Tsumoto, N. Obeyama, Y. Tanaka, Y. Kita, S. N. Timasheff, *Biophys. Chem.* **2007**, *127*, 1-8; b) A. P. Golovanov, G. M. Hautbergue, S. A. Wilson, L. Y. Lian, *J. Am. Chem. Soc.* **2004**, *126*, 8933-8939; c) M. Ishibashi, K. Tsumoto, M. Tokunaga, D. Ejima, Y. Kita, T. Arakawa, *Protein. Expr. Purif.* **2005**, *42*, 1-6; d) K. Tsumoto, D. Ejima, Y. Kita, T. Arakawa, *Protein. Pept. Lett.* **2005**, *12*, 613-619.

[7]   K. Wuthrich, *NMR of Proteins and Nucleic Acids*, Wiley-Interscience, **1986**.

[8]   a) A. Arora, F. Abildgaard, J. H. Bushweller, L. K. Tamm, *Nat. Struct. Biol.* **2001**, *8*, 334-338; b) C. Fernandez, C. Hilty, G. Wider, P. Guntert, K. Wuthrich, *J. Mol. Biol.* **2004**, *336*, 1211-1221; c) F. Hagn, M. Etzkorn, T. Raschle, G. Wagner, *J. Am. Chem. Soc.* **2013**, *135*, 1919-1925; d) J. B. Hartmann, M. Zahn, I. M. Burmann, S. Bibow, S. Hiller, *J. Am. Chem. Soc.* **2018**, *140*, 11252-11260; e) S. Hiller, R. G. Garces, T. J. Malia, V. Y. Orekhov, M. Colombini, G. Wagner, *Science* **2008**, *321*, 1206-1210; f) P. M. Hwang, W. Y. Choy, E. I. Lo, L. Chen, J. D. Forman-Kay, C. R. Raetz, G. G. Prive, R. E. Bishop, L. E. Kay, *Proc. Natl. Acad. Sci. U. S. A.* **2002**, *99*, 13560-13565; g) A. Pautsch, G. E. Schulz, *Nat. Struct. Biol.* **1998**, *5*, 1013-1017; h) M. Renault, O. Saurel, J. Czaplicki, P. Demange, V. Gervais, F. Lohr, V. Reat, M. Piotto, A. Milon, *J. Mol. Biol.* **2009**, *385*, 117-130; i) J. Vogt, G. E. Schulz, *Structure* **1999**, *7*, 1301-1309.

[9]   a) J. U. Bowie, *Curr. Opin. Struct. Biol.* **2011**, *21*, 42-49; b) H. Hong, *Arch. Biochem. Biophys.* **2014**, *564*, 297-313.

[10]   a) J. A. Demmers, J. Haverkamp, A. J. Heck, R. E. Koeppe, 2nd, J. A. Killian, *Proc. Natl. Acad. Sci. U. S. A.* **2000**, *97*, 3189-3194; b) A. Miranker, C. V. Robinson, S. E. Radford, R. T. Aplin, C. M. Dobson, *Science* **1993**, *262*, 896-900; c) O. Nemirovskiy, D. E. Giblin, M. L. Gross, *J. Am. Soc. Mass. Spectrom.* **1999**, *10*, 711-718; d) C. V. Robinson, M. Gross, S. J. Eyles, J. J. Ewbank, M. Mayhew, F. U. Hartl, C. M. Dobson, S. E. Radford, *Nature* **1994**, *372*, 646-651.

[11]   a) P. D. Bosshart, I. Iordanov, C. Garzon-Coral, P. Demange, A. Engel, A. Milon, D. J. Muller, *Structure* **2012**, *20*, 121-127; b) M. Damaghi, S. Koster, C. A. Bippes, O. Yildiz, D. J. Muller, *Angew. Chem. Int. Ed. Engl.* **2011**, *50*, 7422-7424; c) L. Ge, S. Villinger, S. A. Mari, K. Giller, C. Griesinger, S. Becker, D. J. Muller, M. Zweckstetter, *Structure* **2016**, *24*, 585-594; d) J. Thoma, P. Bosshart, M. Pfreundschuh, D. J. Muller, *Structure* **2012**, *20*, 2185-2190; e) J. Thoma, N. Ritzmann, D. Wolf, E. Mulvihill, S. Hiller, D. J. Muller, *Structure* **2017**, *25*, 1139-1144 e1132.

[12]   J. Thoma, B. M. Burmann, S. Hiller, D. J. Muller, *Nat. Struct. Mol. Biol.* **2015**, *22*, 795-802.

Tables

**Table 1. Rate constants of OmpX folding into PC 10:0 liposomes.**

Experimental method	Rate constants
SDS-PAGE[a]	$k_F = 0.0098 \pm 0.00042$ s^{-1}
Fluorescence spectroscopy[a]	$k_F = 0.010 \pm 0.00014$ s^{-1}
ESI-TOF mass spectrometry[b]	$k_H = 0.012 \pm 0.0007$ s^{-1}
Solution NMR spectroscopy[c]	$<k_H(i)> = 0.014 \pm 0.0048$ s^{-1}

[a] Protein folding rate constants, [b] global hydrogen bond formation rate constant, and [c] average residue-specific hydrogen bond formation rate constant with standard deviation.
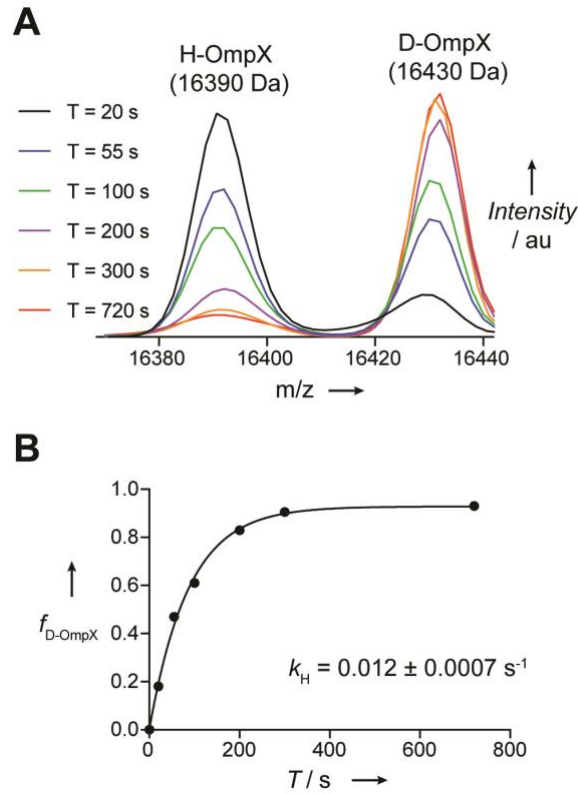
Figures
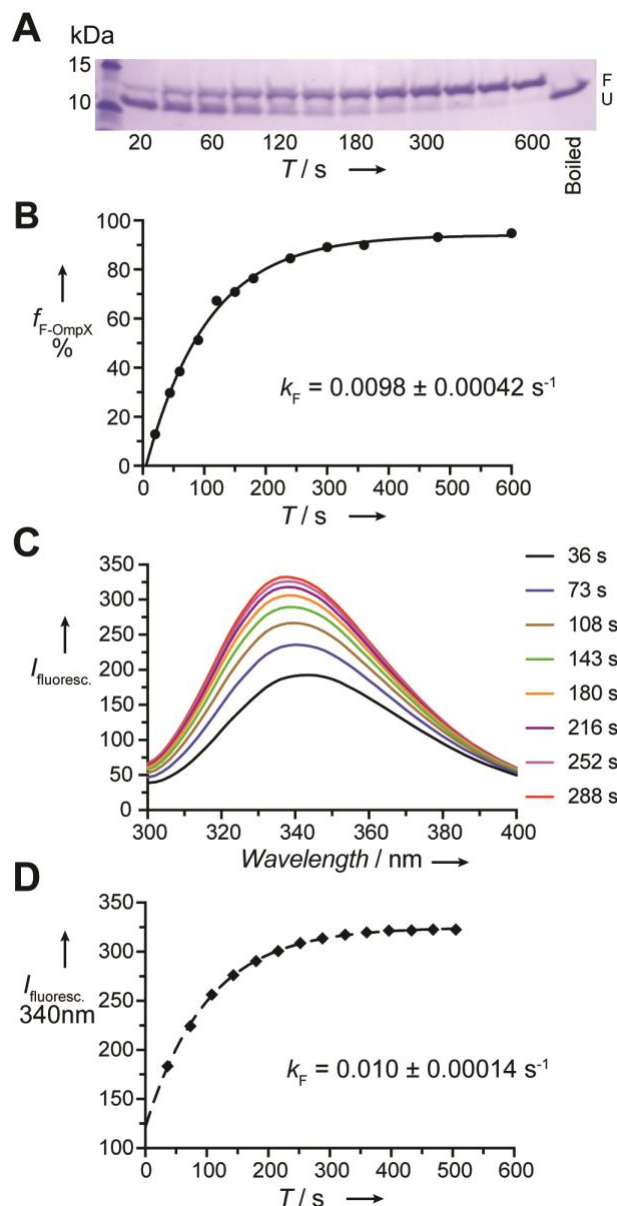
Figure 1. Kinetics of OmpX folding into PC10:0 lipid bilayers. (A) SDS-PAGE gel of the time course of 5.5 µM OmpX folding into PC10:0 liposomes at 25 °C. At the indicated time points, the refolding reaction was quenched and applied to SDS-PAGE. The position of the folded (F) and unfolded (U) species is indicated and a boiled reference sample is shown on the righthand lane. (B) Fraction of folded OmpX as determined from the gel band intensities as a function of the refolding time T. The data (black circles) were fitted with a single exponential (black line). (C) Tryptophan fluorescence spectra of OmpX folding into PC10:0 liposomes under identical buffer conditions as in A. Spectra were recorded at variable time points, as indicated. (D) Time course of the fluorescence intensity at 340 nm. Experimental data (black diamonds) were fitted with a single exponential (black dashed line).
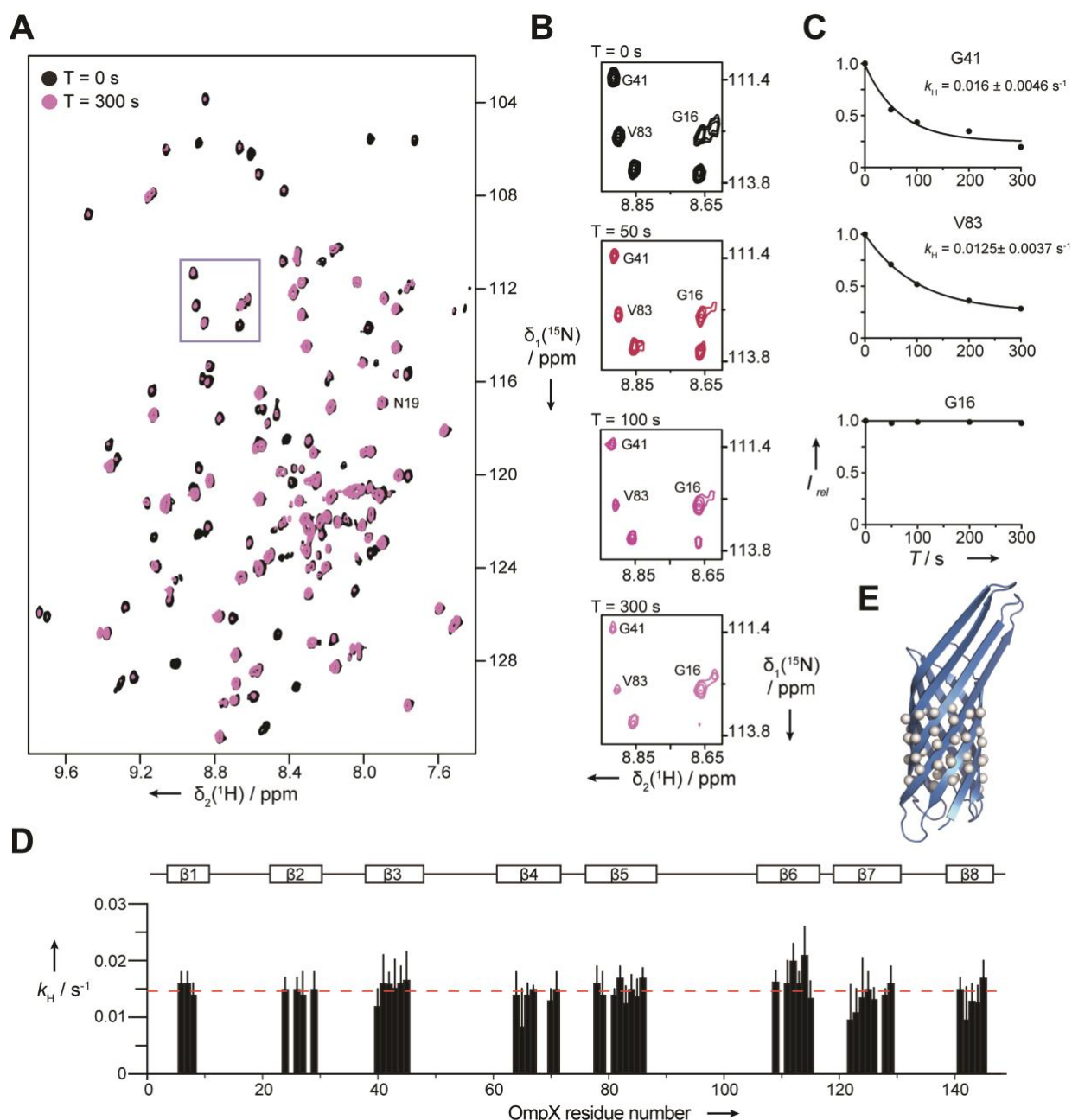
Figure 2. Residue-specific amide hydrogen bond formation kinetics of OmpX refolding into PC10:0 liposomes as monitored by H/D-exchange NMR spectroscopy. (A) 2D [15N,1H]-TROSY spectra of OmpX in LDAO micelles, extracted from a reaction of OmpX refolding into liposomes under H/D exchange conditions with folding times *T* of 0 s (black) and 300 s (purple). Resonance intensities vary due to differential incorporation of deuterium at the backbone amide position. (B) Exemplary spectral region (outlined in grey in A) at variable folding time *T*, as indicated. (C) Relative NMR signal intensities I_{rel} as a function of the refolding time *T* for the residues shown in B. The experimental data (black circles) have been fitted to single exponentials (black lines). (D) Residue-specific hydrogen bond formation rate constants

kH(i) of OmpX folding into PC10:0 liposomes. The red dashed line indicates the average value ⟨kH(i)⟩ of 0.014 $\pm$ 0.0048 s-1. (E) All backbone amide protons of protected residues, for which kinetic hydrogen bond formation data has been obtained, indicated as white spheres on the OmpX crystal structure (PDB 1QJ8). [8i]

Figure 3. Hydrogen bond formation kinetics of individual OmpX molecules refolded into PC10:0 liposomes as monitored by H/D-exchange mass spectrometry. (A) Mass spectra of OmpX folding into liposomes at different folding times T, as indicated. The protonated and deuterated species of OmpX (H-OmpX and D-OmpX, respectively) are labeled. (B) Fraction of the deuterated species, f_{D-OmpX} as a function of the refolding time T. The experimental data (black circles) were fitted with a single exponential (black line).